Available online at www.sciencedirect.com

ScienceDirect

International Journal of Heat and Mass Transfer 51 (2008) 4902–4910

International Journal of HEAT and MASS TRANSFER

www.elsevier.com/locate/ijhmt

Spray water cooling heat transfer at high temperatures and liquid mass fluxes

J. Wendelstorf *, K.-H. Spitzer, R. Wendelstorf

Clausthal University of Technology, Institute of Metallurgy, Robert Koch Strasse 42, D-38678 Clausthal-Zellerfeld, Germany

Received 27 April 2007; received in revised form 17 December 2007
Available online 21 April 2008

Abstract

Spray water cooling is an important technology used in industry for the cooling of materials from temperatures up to 1800 K. The heat transfer coefficient in the so-called steady film boiling regime is known to be a function of the water impact density. Below a specific surface temperature T_L, the heat transfer coefficient shows a strong dependence on temperature (Leidenfrost effect). These findings are the results of complex self-organizing two-phase boiling heat transfer phenomena.

The heat transfer coefficient was measured by an automated cooling test stand (instationary method) under clean (non-oxidizing) surface conditions. Compared to the common thought, an additional temperature dependency in the high temperature regime was found. The heat transfer from the material to the outflowing spray water is explained by a simple model of the two-phase flow region. From the experimental data, an analytic correlation for the dependence of the heat transfer coefficient α as an analytic function of water impact density V_S and temperature ΔT is provided.

For water temperatures around 291 K, surface temperatures between 473 and 1373 K, i.e. $\Delta T > 180$ K and water impact densities between $V_S = 3$ and $30\ \mathrm{kg/(m^2\ s)}$ the heat transfer coefficient α was measured. The spray was produced with full cone nozzles ($v_d \approx 13$–15 m/s, $d_d \approx 300$–$400\ \mu$m).

PACS: 44.35.+c

Keywords: Spray water cooling; Heat transfer coefficient; Full cone nozzle; Subcooled liquid; Film boiling; Continuous casting; Hot rolling

1. Introduction

Spray cooling technology for high temperature surfaces plays an important role in metal production and processing industry. Especially in steel industry, spray cooling is used as secondary cooling procedure in strip casting and for the final microstructure optimization after hot rolling.

The underlying scientific problem is sketched in Figs. 1 and 2. It is characterized by spraying a jet of gas (typically air, characteristic speed v_{air}) containing liquid drops (typically water at a temperature T_W, characteristic volume mean diameter d_d and speed v_d) towards the surface to be cooled. While the technology is applied since the 1940s, scientific investigations started with the theoretical [2] and experimental [9] investigation of film boiling. Spray cooling is investigated since the late 1960s [7,6]. The primary parameter is the temperature of the surface T_S. The water impact density V_S is known to be the second important parameter for the determination of the heat flux. As shown in Fig. 1, every specific water impact density implies a specific boiling curve (from boiling experiments known as Nukiyama [19] curve).

The heat transfer coefficient (HTC) α, defined by $\alpha = q/(T_S - T_W)$ or the heat flux density q itself run through several characteristic regimes. For very low $\Delta T = T_S - T_W$, the heat is transferred through natural convection until

---

* Corresponding author. Tel.: +49 5323 72 2281; fax: +49 5323 72 3120.
E-mail address: jens.wendelstorf@tu-clausthal.de (J. Wendelstorf).
URL: http://www.imet.tu-clausthal.de (J. Wendelstorf).

0017-9310/$ - see front matter © 2008 Elsevier Ltd. All rights reserved.
doi:10.1016/j.ijheatmasstransfer.2008.01.032

Nomenclature

c_p	specific heat (J/(kg K))
d	thickness or diameter (m)
g	acceleration due to gravity (9.81 m/s^2)
r	radius (m)
q	heat flux (W/m^2)
T	temperature (K)
V_S	spray water mass flux (kg/(m^2 s))
v	velocity (m/s)
α	heat transfer coefficient (W/(m^2 K))
β	thermal expansion coefficient (1/K)
ΔT	temperature difference (w/o subscript: $T_S - T_W$) (K)
η	viscosity (Pa s)
λ	heat conductivity (W/(m K))
ρ	density (kg/m^3)
σ	surface tension (N/m)

Dimensionless numbers

Fr	Froude number	$\frac{v}{\sqrt{g \cdot d}}$
Gr	Grashoff number	$\frac{\rho \cdot g \cdot d^3 \cdot \beta \cdot \Delta T}{\eta^2}$
Nu	Nusselt number	$\frac{\alpha \cdot d}{\lambda}$
Pe	Peclet number	$\frac{\rho \cdot c_p \cdot v \cdot L}{\lambda}$
Pr	Prandtl number	$\frac{c_p \cdot \eta}{\lambda}$
Ra	Rayleigh number	$Pr \cdot Gr$
Re	Reynolds number	$\frac{\rho \cdot v \cdot L}{\eta}$
We	Weber number	$\frac{\rho \cdot v^2 \cdot d}{\sigma}$

Subscripts

air	air
d	droplet
f	film fluid (water)
g	gas/vapor
s	sample
S	upper surface (cooled)
U	lower surface (thermocouple)
W	spray water
max	maximum
min	minimum
CHF	critical ((maximum) heat flux)
LF	Leidenfrost point (minimum heat flux)

boiling occurs by the formation of isolated bubbles. These phenomena were described first by Jakob and Linke [12] and are reviewed for the spray cooling case in [3]. In the nucleate boiling regime the vapor bubbles form jets and columns until a maximum (critical) heat flux (CHF) is reached.

Starting the observation from the high temperature regime, a stable vapor film forms between the water film and the surface (film boiling regime [15]). This regime was often characterized by a temperature independent HTC, i.e. the heat flux is linear increasing with ΔT. Our results will demonstrate the deviations from this assumption for higher values of $V_S > 10$ kg/(m^2 s). The minimum heat flux density in the high temperature part of the curve defines the spray cooling Leidenfrost temperature (q_{min}, T_{LF}, see e.g. [28]). Below T_{LF}, the vapor film becomes more

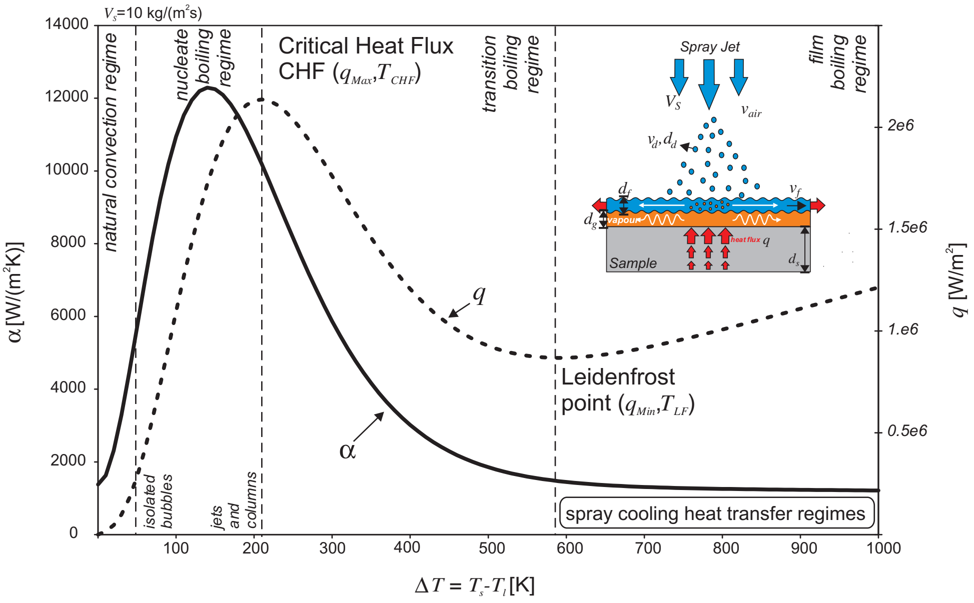

Fig. 1. Spray cooling schema and boiling curve ($V_S = 10$ kg/(m^2 s)).

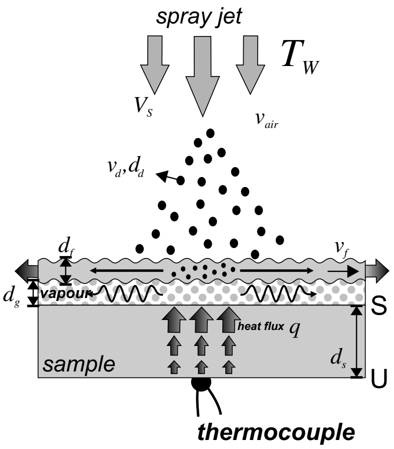

Fig. 2. Cooling scheme.

and more instable until the CHF is reached again. Due to the flooding of the surface, the definition of the Leidenfrost point is different to the original one, which is adapted to droplet evaporation time measurements.

For this paper, water ($T_W = 18$ °C) impact densities from $V_S = 3$–$30\ \mathrm{kg/(m^2\ s)}$ and surface temperatures between 200 and 1100 °C are investigated. The spray was produced with full cone nozzles. From the correlations obtained by Nasr et al. [18], the droplet velocity is $v_d \approx 14\ \mathrm{m/s}$ and the volume mean drop diameter is $d_d \approx 350\ \mu\mathrm{m}$. The experimental data will extend earlier systematic experiments for lower values of V_S and ΔT (e.g. [4,14]) and previous high temperature investigations for lower values of V_S (see e.g. [30] for a correlation analysis).

Before describing the measurements in Section 3 and the resulting correlation for the HTC α in Section 4, some schematic considerations on the two-phase flow phenomena above the hot surface are provided in the next section.

2. General analysis of the two-phase flow region

An *ab-initio* treatment of liquid droplets impacting to a flat hot surface is possible for the limiting case of individual drops splashing directly onto the surface [10] or a surface covered by a liquid film [23]. CFD multiphase VOF models are applicable, but the computational effort required for the parameters of this paper is far from being affordable. For a general insight and for obtaining some qualitative knowledge on the cooling mechanism, a simple model of the heat transfer from the solid surface to the outflowing water is provided here. These calculations will allow a basic understanding of the flow phenomena in the self organized water film and estimates of its characteristic dimensionless numbers.

The vapor film thickness d_g was measured to be between 120 μm at 400 °C and 200 μm at 700 °C ([8], immersion cooling of a 30 mm diameter sphere, $T_W = 55$ °C, $q \approx 0.2\ \mathrm{MW/m^2}$). Thus the heat transport from the surface through the vapor is assumed to be dominated by conduction with some contribution from radiation and convection. The role of the vapor layer is to form a thin skin transporting the energy perpendicular to the surface towards a thin liquid layer. Above the mist cooling regime [26], the impacting liquid droplets are flooding the surface forming this liquid layer of a self organizing mean thickness d_f. In the stationary state, the water film develops an outward velocity v_f and a fluid temperature above that of the impacting spray. The energy is finally carried away by heating the spray water by ΔT_W when it leaves the sprayed region.

For a given water impact density V_S, the mean water film thickness d_f can be estimated by the following assumptions: The film is divided in two regions. The inner region up to the radius r_{max} is dominated by the homogenous spray with the impact density V_S. For radial distances $r > r_{max}$, the flow is assumed to be subcritical, while it is supercritical in the spray region. We try to estimate steady state values for the outflow velocity v_f and the heating provided to the fluid by a given mean HTC α acting in the inner region (as a difference ΔT_W added to the spray water temperature T_W). For the boundary r_{max}, we assume a Froude Number $Fr|_{r=r_{max}} = v_f/\sqrt{g \cdot d_f} \approx 1$. In steady state, the fluid amount provided by V_S flows outward with the velocity v_f at $r = r_{max}$. The amount of vapor penetrating as bubbles through the fluid layer without condensing is assumed to be zero. The model is self consistent for the stable film boiling region. The global mass balance for the inner region is fulfilled by

$$V_S \cdot \pi r_{max}^2 = 2\pi r_{max} \cdot d_f \cdot v_f \cdot \rho_f \tag{1}$$

The $Fr = 1$ condition at r_{max} is equivalent to a Bernoulli equation setting the dynamic pressure $1/2\rho_f \cdot v_f^2$ equal to the average hydrostatic pressure in the fluid layer $1/2\rho_f \cdot g \cdot d_f$.

The values of the fluid layer thickness d_f and the fluid layer outflow velocity v_f can be calculated for given values of r_{max} and V_S

$$d_f = \left(\frac{r_{max} \cdot V_S}{2\rho_f \cdot \sqrt{g}}\right)^{2/3} \tag{2}$$

$$v_f = \left(\frac{g \cdot r_{max} \cdot V_S}{2\rho_f}\right)^{1/3} \tag{3}$$

Finally, the difference ΔT_W between the temperature T_f of the water flowing outward with v_f at r_{max} and the spray water temperature T_W can be calculated for the stationary state. The heat extracted from the material $\alpha \cdot (T_S - T_W) \cdot \pi r_{max}^2$ is equal the heat carried away by the water (with T-increase ΔT_W). In the stationary state, this energy is equal to $V_S \cdot \pi r_{max}^2 \cdot c_{p,f} \cdot \Delta T_W$. As a result, ΔT_W can be calculated by

$$\Delta T_W = \frac{\alpha \cdot (T_S - T_W)}{V_S \cdot c_{p,f}} \tag{4}$$

The fluid properties are taken for water between 18 and 95 °C ($\rho_f = 959$–$998\ \mathrm{kg/m^3}$, $c_{p,f} = 4182\ \mathrm{J/(kg\ K)}$, $\lambda_f = 0.60$–$0.68\ \mathrm{W/(m\ K)}$, $\eta_f = 0.28$–$1\ \mathrm{mPa\ s}$, $\beta_f = 21$–$74 \times 10^{-5}\ \mathrm{K^{-1}}$

and $\sigma = 59$–72 mN/m). Using two representative values for α in the film boiling regime at $V_S = 3$ and 30 kg/(m^2 s) and three representative values for the radius of the sample or sprayed area, the water film thickness d_f, the outflow velocity v_f and ΔT_W are provided in Table 1. The slow variation of $\Delta T_W \approx 20$ K explains the experimental findings on the HTC dependency on water temperature [24,22]. The two-phase system behaviour is similar for water temperatures from 20 to 60 °C, while above ≈80 °C, the heating of the liquid phase is limited by the onset of boiling. Thus the model explains the small changes of the HTC with water temperatures below ≈60 °C while the HTC decreases at higher water temperatures or lower subcooling degrees respectively. The spray water temperature is thus not varied in the experiments.

This simple model provides realistic ranges for the values of the water film parameters and allows to calculate the characteristic numbers for the fluid flow in the liquid layer ($r = 1/2r_{max}$). The Reynolds number is above $Re_f = 13$ but presumably in the laminar regime. Only for high spray water temperatures and high water impact densities Re_f can be above 1000. The Weber number is small ($We_f < 0.6$), i.e. surface tension dominates viscosity in the water film. The Grashoff Gr_f number is well above 1, i.e. inertia and buoyancy forces are again more important than viscosity. The Peclet numbers are much greater than unity thus the assumption of a pure convective heat transport in the liquid film is self consistent. Momentum diffusity dominates thermal diffusity ($Pr_f = 1.7$–7). Rayleigh numbers in the film can reach critical values in principle, but the formation of Benard cells is thought to be inhibited by the radial outward flow.

For the stable steam layer forming in the film boiling regime, the gas properties strongly depend on temperature. The values are taken for hot steam at atmospheric pressure between 100 and 500 °C ($\rho_g = 0.17$–0.59 kg/m^3, $c_{p,g} = 2077$–2478 J/(kg K), $\lambda_g = 0.025$–0.136 W/(m K), $\eta_g = 0.012$–0.048 mPa s and $\beta_g = 0.8$–2.9×10^{-3} K^{-1}). In the steam layer ($Pr_g = 0.18$–4.7, $Gr_g < 0.4$), the energy transport (Benard problem, see e.g. [5]) is presumably dominated by conduction, because it is too thin to develop convection cells between the hot solid surface $T = T_S$ and the phase boundary $T = T_{sat} \approx 100$ °C ($Ra_g < 2$). Due to the nonequilibrium nature of the steam layer, its mean temperature and thus heat conductivity is high ($\lambda_g \approx 0.08$ W/(m K) [13]). A HTC value of typically 1000 W/(m^2 K) can be explained by pure heat conduction for a layer thickness below 80 μm.

Table 1
Values of the fluid layer thickness d_f, outflow velocity v_f and temperature difference ΔT_W at a surface temperature of $T_S = 600$ °C, $T_W = 18$ °C and typical α values for low ($V_S = 3$ kg/(m^2 s)) and high spray intensity ($V_S = 30$ kg/(m^2 s))

α (W/m^2 K)	r_{max} (mm)	d_f (mm)	v_f (m/s)	ΔT_W (K)
425	10	0.28	0.053	19.7
425	20	0.45	0.067	19.7
425	50	0.83	0.090	19.7
3616	10	1.32	0.114	16.8
3616	20	2.09	0.143	16.8
3616	50	3.86	0.194	16.8

The conventional Nusselt number approach is not used here, because the required length (d_g) and heat conductivity (λ_g) can not be measured, while the HTC α can be directly measured.

The droplets of industrial sprays usually show very high Weber numbers, i.e. they reach the liquid layer surface in a highly deformed inhomogeneous state. For the sprays used in this paper, the droplet Weber number is approximately $We_d = 1000 \pm 500$.

The most problematic approximation may be the missing momentum balance (using the $Fr = 1$ boundary condition) which is difficult to solve due to the required temporal and spatial resolution (droplet impact) required for a VOF–CFD model in a calculation domain of more than 20x2 mm.

3. Experimental methods

The HTC measurements were done for the horizontal spray position (spraying downwards, see Fig. 3). The water impact density was measured in advance for different nozzles depending on the nozzle-sample distance [27]: Replacing the heat transfer sample by measuring cups of different diameters, V_S is derived from $V_S = m/(A \cdot t)$, where m is the water mass in the cup (area A) after time t. Using this method, the values of V_S are accurate by ±8% (systematic measurement accuracy and statistical fluctuations). Full cone nozzles (Spraying Systems VKE6/60, VKE6/90 and VKE8/60) were used at spraying distances ranging from 62 to 105 mm. The droplet velocity and size distributions where not directly measured but obtained from correlations found in the literature [18]. For the spray parameters used, the possible values of the average droplet velocity is calculated to be 13–15 m/s and the mean diameter is in the range of 300–400 μm for the values of the impingement density under investigation.

The sheet specimens of commercially pure nickel (99.3% Ni) with a thickness of 1.0 mm were milled to discs with 70 mm in diameter. Up to 5 thermocouple pairs, one in the center and the others perpendicular at a radius of 10 mm, were spot welded to the lower side of the sample discs. The temperature measurement was carried out with Ni–CrNi thermocouples with a wire diameter of 0.5 mm. The thermocouple wires were insulated by thin ceramic tubes. Supported by heat conduction calculations for the complete sample holder, there were no differences in the cooling curves for the different thermocouple positions and thus no radial heat transport. The experimental set-up sketched in Fig. 3 was used for heating the samples and measurement of the sample temperature during spray cooling.

After installation in the furnace sample holder, the disks were heated under protective atmosphere up to 1200 °C. Reaching the test temperature, the sample was moved

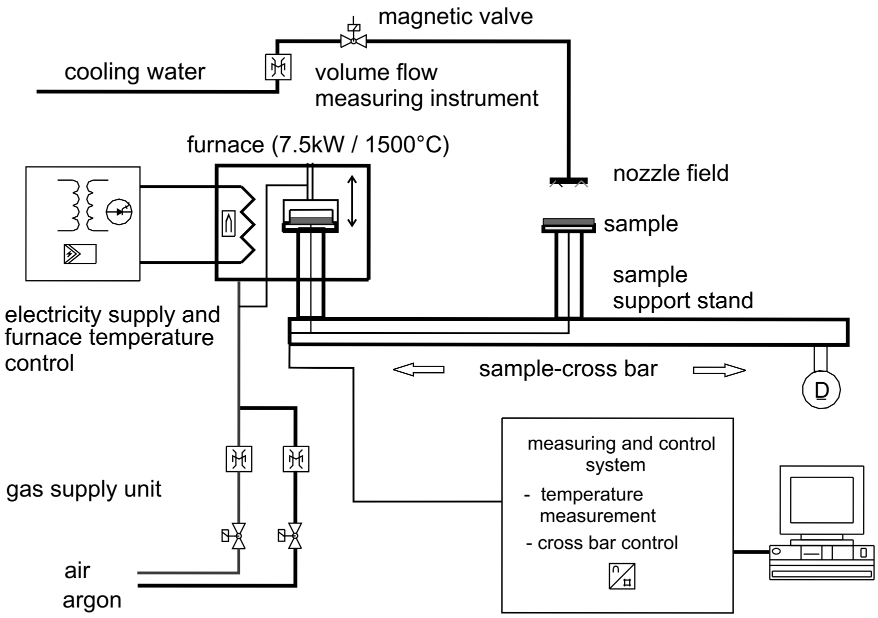

Fig. 3. Experimental set-up.

automatically from the furnace under the full cone nozzle, which takes approximately 4 s. In this position, it is subsequently cooled with spray water (mass flux density V_S). The water temperature T_W was approximately 18 °C. The resulting measurement data is the time depending temperature for the individual thermocouples welded to the back of the samples ($\Delta t = 0.1$ s, $\Delta T = 0.75\%/2.5$ K).

Copper was not taken as sample material because of the lower melting point and due to problems with soldering or welding the thermocouples. Different steels were tested showing equivalent results within the measurement accuracy. It has to be noted, that in the case, the sample material undergoes phase transformations during cooling – like steel materials below 900 °C – the accuracy is limited by the unknown exact values of $c_p(T)$.

3.1. Analysis and measurement accuracy

In principle, the heat transfer coefficient due to spray water cooling does not depend on the material to be cooled. Apparent significant material dependencies can be explained by the effect of differing surface conditions or differing surface cooling rates in the order of magnitude of the time scales required by the water film to adapt to changes in the surface temperature. For technically pure nickel, there are no unpredictable phase transformations occurring in the temperature range under consideration. The specific heat capacity depending on temperature $c_p(T)$ was calculated with the Thermo-Calc Software based on the chemical analysis [25].

Additionally, the nickel surface structure is not affected by high temperatures up to 1700 K. The very thin protective oxide layer forming at higher temperatures was not crucial due to its stability and thickness (see [29] for a discussion of the oxide layer effects).

The cooling conditions are sketched in Fig. 2. For thin samples, the temperature differences between the surface S and the backside U (≈10 K in the stable film boiling regime) are small and the cooling rate at positions S and U is nearly the same. The heat transfer coefficient can be directly derived from the measured values $T_U(t)$ (for details see [27])

$$\alpha \approx -\frac{c_p(T_U)\cdot\rho_S\cdot d_S}{T_U - T_W}\cdot\left.\frac{\partial T_U}{\partial t}\right|_U \tag{5}$$

The results from Eq. (5) are identical to those obtained by a more computationally intense inverse modelling analysis. The measurement accuracy can be calculated from the error propagation law using the accuracies of the values required in Eq. (5). The specific heat data has an absolute accuracy of about 8% [20], the temperature accuracy was taken from the type K thermocouple specifications (IEC-584-2) and the accurate determination of the cooling rate $\partial T_U/\partial t$ was performed by numerical techniques [27]. The cooling rate was obtained with an accuracy of 8%. An additional error of 2% comes from the $\rho_s \cdot d_s$ product due to thermal expansion of the sample. In the stable film boiling region, the overall systematic accuracy for the determination of α was 11% and the statistical fluctuation was found to be around 5–8% as long as the spray nozzles are not introducing additional fluctuations due to operating them beyond their stable parameter settings. In the transition boiling regime, statistical fluctuations can be up to 30%. Due to the high and time dependant cooling rates below the Leidenfrost temperature T_L, the α-measurement accuracy is estimated to be 10–30% in this area.

4. Experimental results

For water mass flux densities varying from 3 to 30 kg/(m^2 s) and temperature differences from 150 to 1100 K the cooling curves were measured (28 experiments, 73 cooling curves). The examples shown in Fig. 4 demonstrate the well known principal behaviour. The cooling rate in the stable film boiling regime increases with increasing water mass flux density V_S. The onset of transition boiling (Leidenfrost point) can be identified by the lower temperature bending of the cooling curve. The high temperature bend in the cooling curves is due to the onset of cooling when the sample reaches the spray position. For this reason, the α calculation should start well below the furnace temperature to avoid artificial low α-values at high temperatures. For this reason, the experiments where repeated with different starting temperatures and only the data not depending on the starting temperatures are used.

4.1. Boiling curve correlation

From the HTC values α calculated by Eq. (5) from all experimental data sets, the $\alpha(V_S, \Delta T)$-dependency was determined in form of an analytic correlation formula (the ±-values indicate the 95%-confidence intervals)

$$\begin{aligned}\alpha(\Delta T,\ V_S) = 190 \pm 25 + \tanh\left(\frac{V_S}{8}\right) \\ \times\left(140 \pm 4 \cdot V_S\left[1 - \frac{V_S \cdot \Delta T}{72{,}000 \pm 3500}\right]\right. \\ \left. + 3.26 \pm 0.16 \cdot \Delta T^2\left\{1 - \tanh\left(\frac{\Delta T}{128 \pm 1.6}\right)\right\}\right)\end{aligned} \quad (6)$$

Compared to equivalent correlations for the Nusselt heat transfer number this fit-formula has the important advantage of a direct practical applicability, while the dimensionless numbers require values for a number of unknown quantities like the vapor layer thickness or the mean velocity in the liquid layer (see Section 2).

This correlation is visualized in Fig. 5. Compared to the literature, this correlation is valid for all boiling regimes (no piecewise definition). The high temperature values ($\Delta T > 400$ K) are in agreement with the extrapolated data from existing correlations [17].

In the stable film boiling regime at $\Delta T = 700$ K data from other references is available. Eq. (6) is found to be in good agreement with the independent measurement data from these references (see Fig. 6). As long as the measurement accuracy was specified or can be determined from the data provided, the correlation agrees within the error limits [27].

In the low temperature regime $\Delta T < 400$ K, there are quantitative deviations from the data of other groups, which can be explained by the different spray parameters and the larger experimental error in this parameter range. Nevertheless, for ΔT in the CHF regime and below Eq. (6) shows the correct qualitative behaviour allowing the application of this correlation to heat transfer problems where accurate results are required in the high temperature regime without getting any unphysical or qualitatively wrong results below the Leidenfrost point (numerical stability). The discontinuities from piecewise defined correlations beyond their extrapolation limits are thus avoided.

Finally the correlation given in Eq. (6) provides quantitative values for the additional α dependency on ΔT for water mass flux densities above $V_S = 10$ kg/(m^2 s). As shown in Figs. 7 and 5, the formerly postulated ΔT-independency in the high ΔT-regime may come unavailability of reliable data above $\Delta T = 700$ K. Our experiments were found to be accurate up to $\Delta T \approx 1100$ K and the HTC

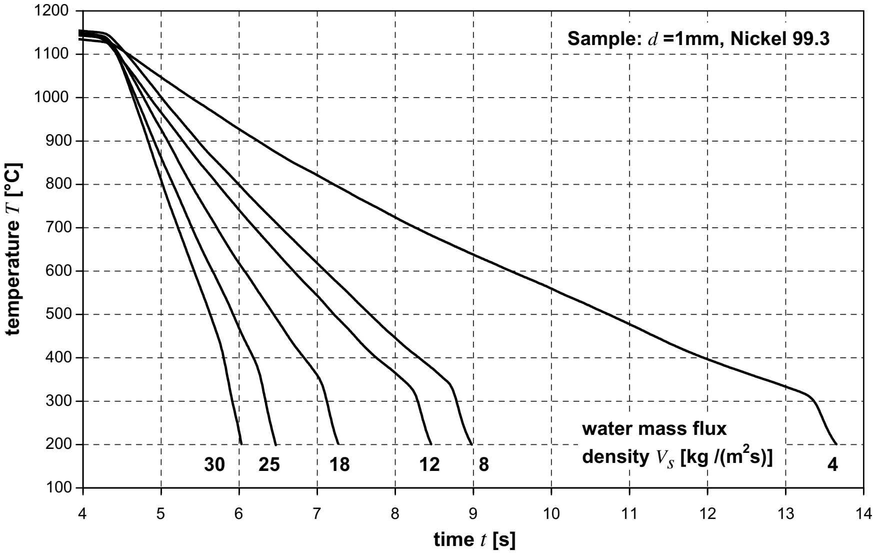

Fig. 4. Cooling curves.

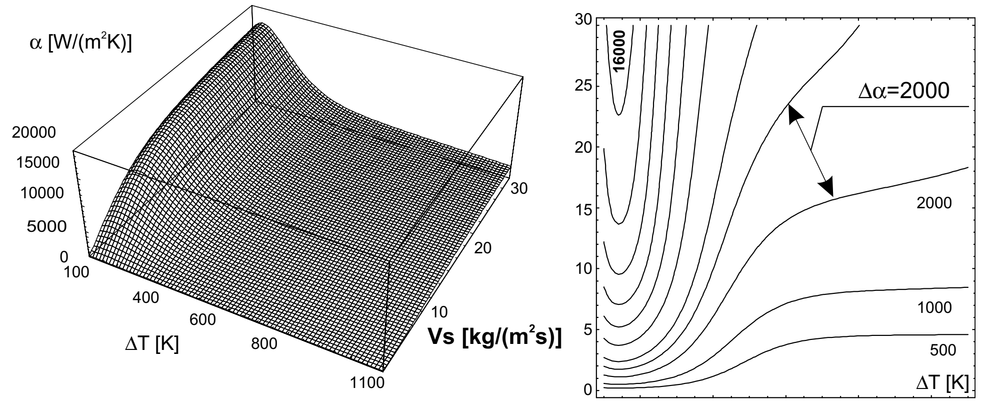

Fig. 5. Heat transfer coefficient correlation (Eq. (6)).

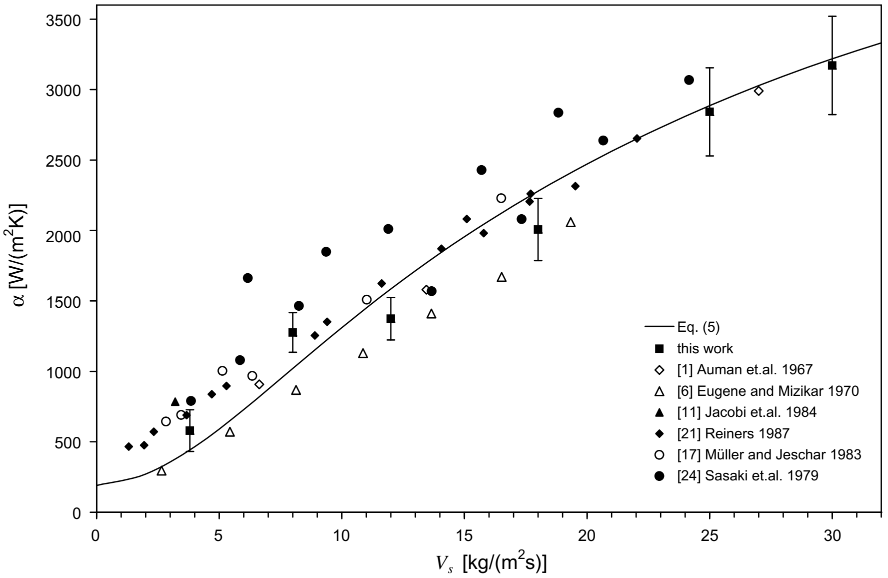

Fig. 6. HTC depending on V_S for $\Delta T \approx 700$ K. See above mentioned references for further information.

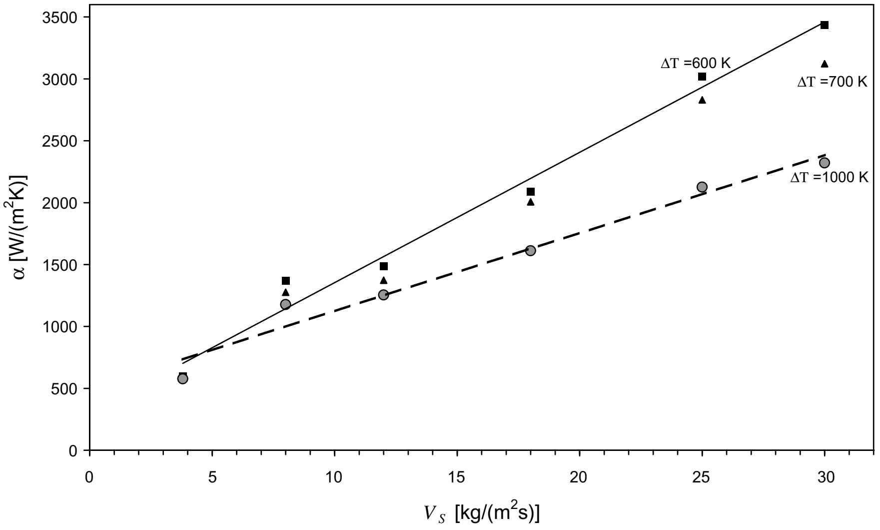

Fig. 7. HTC depending on V_S for different values of ΔT.

decrease shown in Fig. 7 is significant and important for the prediction of steel mass production cooling processes, where such high values of ΔT are normal. The experimental evidence of this phenomenon was judged to be significant. For a detailed explanation, advanced modelling and more high temperature experiments may be useful. Because of the lower heat conductivity of the vapor layer for higher ΔT, the observations are compatible with the concept of *stable* film boiling.

5. Summary and conclusions

The heat transfer for spray cooling of clean surfaces using full cone nozzles ($v_\mathrm{d} \approx 14$ m/s, $d_\mathrm{d} \approx 350$ μm) in the parameter range $V_\mathrm{S} = 3$–30 kg/(m^2 s) and surface temperatures between 200 and 1100 °C were investigated. The resulting correlation includes the full ΔT and V_S-dependency of the heat transfer coefficient α:

- The stable film boiling regime shows an HTC decreasing with temperature difference for $V_\mathrm{S} > 10$ kg/(m^2 s) and ΔT above $\approx$800 K (Fig. 7).
- The absolute accuracy of the HTC measurement was better than 11% in the film boiling regime.

For the transition regimes between mist cooling and (flooding) spray cooling ($V_\mathrm{S} = 0.1$–5 kg/(m^2 s)), additional experiments may be required to enhance the accuracy of existing correlations [17]. For the very high mass flux density regime ($V_\mathrm{S} > 20$) the details of the transition to jet cooling may require further investigations. For the validation of modelling data and for industrial cooling system optimization, the measurement accuracy requires further enhancement, especially below the Leidenfrost temperature.

Acknowledgements

This work was supported by the German Ministry of Commerce (BMWA) under the supervision of the AiF member society *VDEh Gesellschaft zur Förderung der Eisenforschung* under Ref. No. 139133N. We express our gratitude to the financial supporters, to the industrial steering committee of the project and to our technicians, especially to H. Hillebrecht with his outstanding long term experience in the field of HTC measurement. The work was performed as a cooperation of the Institute for Energy Process Engineering and Fuel Technology (Univ.-Prof. Dr.-Ing. R. Scholz and Univ.-Prof. Dr.-Ing. R. Weber) and the Process Metallurgy Group (Univ.-Prof. Dr.-Ing. K.-H. Spitzer) at the Institute of Metallurgy, both at Clausthal University of Technology, Germany.

References

[1] P.M. Auman, D.K. Giffiths, D.R. Hill, Hot strip mill runout table temperature control, Iron Steel Eng. (September) (1967) 174–179.
[2] L.A. Bromley, Heat transfer in stable film boiling, Chem. Eng. Progr. 46 (5) (1950) 221–227.
[3] L.C. Chow, M.S. Sehmbey, M.R. Pais, High heat flux spray cooling, Ann. Rev. Heat Transfer 8 (1997) 291–318.
[4] S. Deb, S.C. Yao, Analysis on film boiling heat transfer of impacting sprays, Int. J. Heat Mass Transfer 32 (11) (1989) 2099–2112.
[5] W.R. Debler, The Onset of Laminar Natural Convection in a Fluid with Homogeneously Distributed Heat Sources, PhD thesis, University of Michigan, 1959.
[6] A. Eugene, A. Mizikar, Spray cooling investigation for continuous casting of billets and blooms, Iron Steel Eng. 47 (6) (1970) 53–60.
[7] R.E. Gaugler, An Experimental Study of Spray Cooling of High Temperature Surfaces, PhD thesis, Department of Mechanical Engineering, Carnegie Institute of Technology, Pittsburg, PV, 1966.
[8] V. Heidt, Berechnung der Wärmeübertragung und der Dampffilmdicke beim stabilen Filmsieden mit freier Konvektion, PhD thesis, Technische UniversitSt Clausthal, 1993.
[9] E.R. Hosler, J.W. Westwater, Film boiling on a horizontal plate, ARS J. 32 (4) (1962) 553–558. April.
[10] R.J. Issa, S.C. Yao, A numerical model for the mist dynamics and heat transfer at various ambient pressures, J. Fluids Eng. (Trans. ASME) 127 (4) (2005) 631–639, July.
[11] H. Jacobi, G. Kaestle, K. Wünnenberg, Heat transfer in cyclic secondary cooling during solidification of steel, Ironmak. Steelmak. 11 (3) (1984) 132–145.
[12] M.L. Jakob, W. Linke, Der Wärmeübergang von einer waagerechten Platte an siedendes Wasser, Forschung auf dem Gebiete des Ingenieurwesens 4 (March/April) (1933) 75–81.
[13] F.G. Keyes, The viscosity and heat conductivity of steam, J. Am. Chem. Soc. 72 (1) (1950) 433–436, doi:10.1021/ja01157a116.
[14] W.P. Klinzing, J.C. Rozzi, I. Mudawar, Film and transition boiling correlations for quenching of hot surfaces with water sprays, J. Heat Treat. (USA) 9 (2) (1992) 91–103.
[15] J.G. Leidenfrost, On the fixation of water in diverse fire, Int. J. Heat Mass Transfer 9 (1966) 1153–1166, translated from anno 1756 original.
[16] I. Mudawar, W.S. Valentine, Determination of the local quench curve for spray-cooled metallic surfaces, J. Heat Treat. (USA) 7 (2) (1989) 107–121.
[17] H.R. Müller, R. Jeschar, Wärmeübergang bei der Spritzwasserknhlung von Nichteisenmetallen, Zeitschrift fnr Metallkunde 74 (5) (1983) 257–264.
[18] G.G. Nasr, R. Sharief, D.D. James, J.R. Jeong, Studies of high pressure water sprays from full cone atomizers, in: ILASS-Europe'99, Toulouse 5–7 July 1999, 1999, pp. 1–6.
[19] S. Nukiyama, Maximum and minimum values of heat q transmitted from metal to boiling water under atmospheric pressure, Nihon-Kikai-Gakkai-shi (J. Jpn. Soc. Mech. Eng.) 37 (1934) 367–374, translation in IJHMT 9 (1966) 1419.
[20] W. Obendrauf, E. Kaschnitz, G. Pottlacher, H. Jäger, Measurements of thermophysical properties of nickel with a new highly sensitive pyrometer, Int. J. Thermophys. 14 (3) (1993) 417–426.
[21] U. Reiners, Wärmeübertragung durch Spritzwasserkühlung heißer Oberflächen im Bereich der stabilen Filmverdampfung, PhD thesis, Technische Universität Clausthal, 1987.
[22] U. Reiners, R. Jeschar, R. Scholz, Heat transfer during continuous casting cooling because of spray water, Steel Res. 60 (10) (1989) 442–450.
[23] I.V. Roisman, C. Tropea, Impact of a drop onto a wetted wall: description of crown formation and propagation, J. Fluid Mech. 472 (2002) 373–397.
[24] K. Sasaki, Y. Sugatani, M. Kawasaki, Heat transfer in spray cooling on hot surface, Tetsu-to-Hagane (J. Iron Steel Inst. Jpn.) 65 (January) (1979) 90–96.

[25] B. Sundman, P. Shi, Thermo-Calc Software, <http://www.thermo-calc.se>, 2004. Version Q.

[26] S. Toda, A study of mist cooling/1st report – Investigation of mist cooling, Heat Transfer – Jpn. Res. 1 (3) (1972) 39–50, July–September.

[27] R. Viščorová, Untersuchung des Wärmeübergangs bei der Spritzwasserkühlung unter Berücksichtigung des Einflusses der Verzunderung, PhD thesis, Technische UniversitSt Clausthal, 2007, <http://www.gbv.de/dms/clausthal/E_DISS/2007/db108527.pdf>.

[28] R. Weber, Lecture Notes in Heat Transfer, International Studies in Science and Engineering, Papierflieger, Clausthal-Zellerfeld, 2004.

[29] R. Wendelstorf, K.H. Spitzer, J. Wendelstorf, Effect of oxide layers on spray water cooling heat transfer at high surface temperatures, Int. J. Heat Mass Transfer 51, (2008), accepted for publication, doi:10.1016/j.ijheatmasstransfer.2008.01.033.

[30] S.C. Yao, T.L. Cox, A general heat transfer correlation for impacting water sprays on high-temperature surfaces, Exp. Heat Transfer 15 (4) (2002) 207–219.